nature nanotechnology

LETTERS

PUBLISHED ONLINE: 30 SEPTEMBER 2012 | DOI: 10.1038/NNANO.2012.165

Photocurrent of a single photosynthetic protein

Daniel Gerster[1], Joachim Reichert[1]*, Hai Bi[1], Johannes V. Barth[1], Simone M. Kaniber[2], Alexander W. Holleitner[2], Iris Visoly-Fisher[3], Shlomi Sergani[3] and Itai Carmeli[4]*

Photosynthesis is used by plants, algae and bacteria to convert solar energy into stable chemical energy. The initial stages of this process—where light is absorbed and energy and electrons are transferred—are mediated by reaction centres composed of chlorophyll and carotenoid complexes[1]. It has been previously shown that single small molecules can be used as functional components in electric[2–6] and optoelectronic circuits[7–10], but it has proved difficult to control and probe individual molecules for photovoltaic[11–13] and photoelectrochemical applications[14–16]. Here, we show that the photocurrent generated by a single photosynthetic protein—photosystem I—can be measured using a scanning near-field optical microscope set-up. One side of the protein is anchored to a gold surface that acts as an electrode, and the other is contacted by a gold-covered glass tip. The tip functions as both counter electrode and light source. A photocurrent of ~10 pA is recorded from the covalently bound single-protein junctions, which is in agreement with the internal electron transfer times of photosystem I.

In our set-up, photosystem I (PS I) was covalently bound to the substrate and metallized scanning near-field optical microscopy (SNOM) tip via cysteine mutation groups (Fig. 1; see Supplementary Methods)[13,17–19]. Photoexcitation of PS I triggers a series of redox reactions in which an electron is transferred along the reaction-centre electron transfer chain with an internal quantum efficiency close to 1 (ref. 1). We used bipolar mutants of PS I, where the mutations are located at both the oxidizing (red arrows in Fig. 1c) and reducing sides (grey arrow in Fig. 1c) of the PS I. The cysteine groups promote an oriented self-assembly of the PS I on surfaces as well as good electronic coupling between the PS I and the electrodes. For control measurements, we utilized unipolar mutants of PS I with two cysteine groups only on the oxidizing side (red arrows in Fig. 1c). The unipolar PS I has no cysteine mutation on the reducing side of the electron pathway.

The SNOM tip comprises a macroscopic, tetrahedral glass fragment with an atomically sharp apex (for a detailed description see Supplementary Methods). The glass fragment is metallized by a thin gold film. The distance between the substrate and the SNOM tip is controlled by a single high-resolution piezoelectric element (Supplementary Fig. S2). The tip is illuminated from the back side of the glass fragment by 633 nm laser light with a power of ~4 mW. In this way, a highly efficient coupling of the incident beam to a local excitation of the tip apex and the PS I is achieved.

Generally, the PS I complex consists of 12 polypeptides, to which 96 light-harvesting chlorophyll and 22 carotenoid pigment molecules are bound[1]. The PS I protein has a cylindrical shape with a diameter of ~15 nm and a height of 9 nm. After photoexcitation of the special pair of chlorophyll (P700) an electron is transferred to a monomeric chlorophyll (Chl) at ~1 ps (Fig. 2). The excited electron relaxes via two intermediate phylloquinones to three [4Fe–4S] iron–sulphur centres. The first iron cluster (F_X) is located just outside the molecular electron transfer chain, and the transfer rate from the phylloquinones to F_X is biphasic with time constants of ~15–150 ns. The electron is then transferred to the last two iron clusters $F_{A/B}$ in less than 500 ns.

Figure 3a shows a typical dark current versus distance profile at $V_{bias} = 0.25$ V when the tip approaches a submonolayer of bipolar PS I from 12 nm down to a metallic contact with the substrate in an ultrahigh-vacuum environment at room temperature. We distinguish two different conductance regimes. Between 9 and 3 nm, we detect a finite current of ~300 pA with fluctuations of ~200 pA. Below 3 nm, the current increases rapidly in a

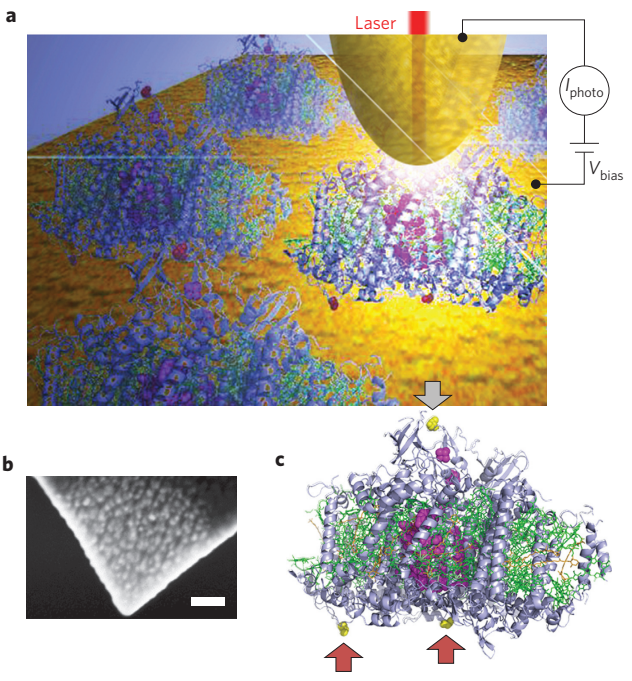

Figure 1 | Measuring the photocurrent of a single PS I. a, Photocurrent I_{photo} is determined following covalent bonding of a gold-covered glass tip to an individual PS I and optically exciting the PS I with a laser from the back of the tip. **b**, Scanning electron microscope (SEM) image of such a tip made from SiO_2 and covered with ~20 nm of gold. Scale bar, 100 nm. **c**, Molecular structure image of PS I based on crystallographic data. PS I is composed of polypeptide chains (grey) in which chlorophyll (green) and carotenoids (orange) are embedded. The chromophores that mediate the electron transfer are represented by the space fill model (magenta). The PS I can covalently bind to the tip and substrate through cysteine mutations (arrows).

[1]Physik-Department E20, Technische Universität München, James-Franck Strasse, D-85748 Garching, Germany, [2]Walter Schottky Institut and Physik-Department, Technische Universität München, Am Coulombwall 4a, D-85748 Garching, Germany, [3]Department of Chemistry and Ilse Katz Institute for Nano-scale Science and Technology, Ben Gurion University of the Negev, Be'er Sheva 84105, Israel, [4]Center for NanoScience and Nanotechnology and School of Chemistry, Tel Aviv University, Tel Aviv 69978, Israel. *e-mail: joachim.reichert@tum.de; itai@post.tau.ac.il

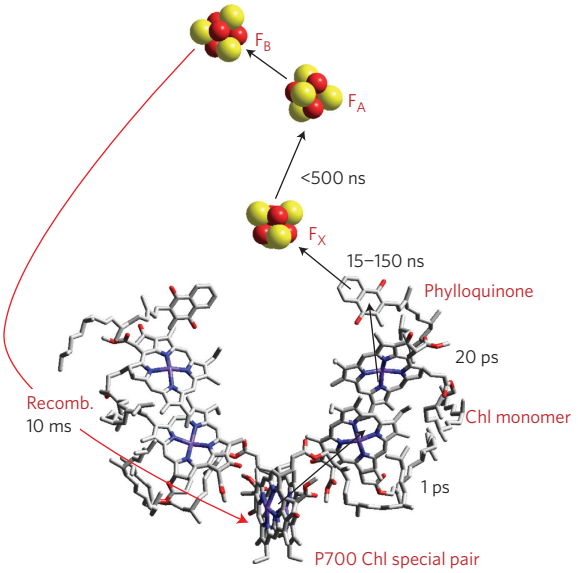

Figure 2 | The reaction-centre electron transfer chain, showing electron transfer and recombination times. After photoexcitation of an electron in the chlorophyll (P700) special pair, the electron is transferred to three [4Fe-4S] iron-sulphur clusters.

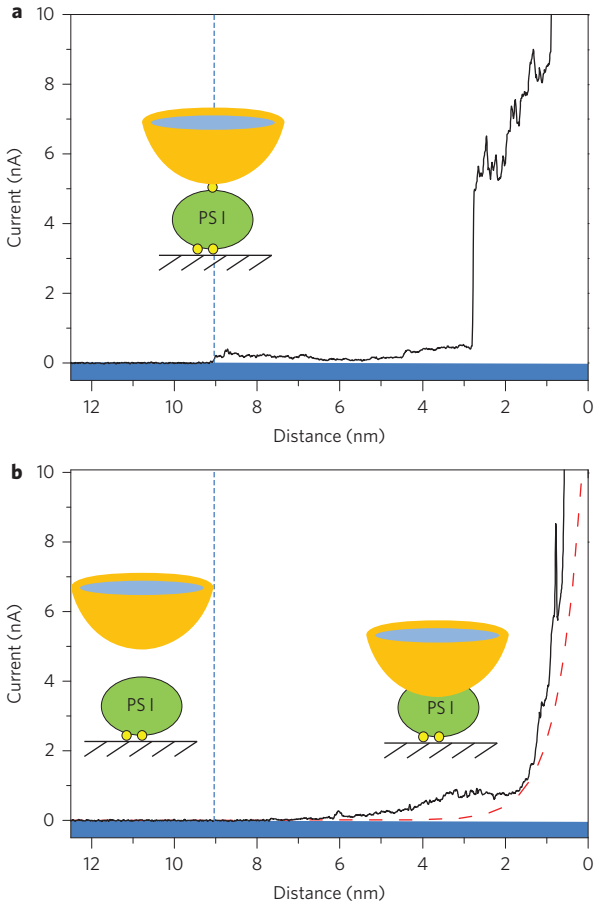

Figure 3 | Current versus gap distance profiles. a, Profile for a submonolayer of bipolar PS I measured in ultrahigh vacuum at $V_{bias} = 0.25$ V. **b**, As in **a**, but for a submonolayer of unipolar PS I. The red curve shows measured vacuum tunnelling without photosystems on the substrate. The schematics in **a** and **b** illustrate the different contact regimes between the tip (yellow), the PS I (green) and the substrate.

non-systematic manner until a metallic contact is formed (zero distance). The current fluctuations always occur after we first touch the molecule and then push the apex of the tip into the soft protein. We note that beyond the point where the first fluctuations emerge, the current–distance dependence is irreversibly modified: when the tip–sample distance is again increased after touching a protein, the tip has to be retracted by more than 50 nm until the current through the molecule eventually fades out (not shown). This is associated with the protein being covalently linked to the tip. Upon tip retraction, the protein unfolds until finally the contact is broken. In our experiments, the tip was replaced every time it came into contact with a protein. For control, we also characterized unipolar proteins assembled on the substrate. A typical approach curve is presented in Fig. 3b. A 'lock in' behaviour at ~9 nm above the surface (as seen for the bipolar PS I), where the tip is at the height of the protein layer, was never observed for the unipolar PS I species. We do not see a significant deviation from an experimentally observed vacuum-like tunnelling behaviour (dotted red line in Fig. 3b) at this height. Instead, we observe a shoulder-like feature much closer to the surface. At this point, the tip is assumed to deform the protein layer strongly, without forming any covalent bonds.

For both bipolar and unipolar PS I, the current–voltage characteristics were recorded at tip–surface distances below the point where the first fluctuations appeared in the current–distance curve. The proteins were approached with an illuminated tip or a dark tip, and the light was not switched on or off during photocurrent measurements. For a low bias voltage, $|V_{bias}| < 50$ mV, the molecular junctions show a linear current–voltage dependence (Fig. 4a). For $|V_{bias}| \geq 0.5$ V, the characteristics become more and more nonlinear (Fig. 4a, inset). Nonlinear characteristics have been reported both for transport across single reaction centres without laser excitation[11,20,21] and for corresponding photoconductance–voltage characteristics[22,23].

To determine a value for the photocurrent, the current–voltage characteristics under light excitation were fitted linearly for $|V_{bias}| \leq 20$ mV. These fits were analysed for their residual current at zero bias (short-circuit current), which we define as I_{photo}. The histograms of I_{photo} in Fig. 4b show the accumulated photocurrent measurements for samples of the bipolar PS I, which exhibit positive (red) and negative (blue) offsets. The different signs of I_{photo} are attributed to the two possible orientations of the bipolar PS I with respect to the applied bias direction. The average value of the photocurrent of six junctions in 77 measurements was 9.8 ± 5.1 pA, irrespective of the direction. The photocurrent fluctuations remain at the same order of magnitude between subsequent measurements. These strong fluctuations, which do not exist in the absence of the PS I layer (green histogram), suggest that the tip is in contact with the PS I, as previously concluded in similar single-molecule experiments exploiting mechanically controlled break junctions[3,24]. The fluctuations are also present when the tip is in contact with a bipolar PS I without illumination (black histogram), but this distribution does not show a significant offset in the residual current. We consider a junction to be exhibiting a 'significant' photocurrent when the mean value of the residual current in a sequence of measurements is larger than its standard deviation (for more information, see Supplementary Notes). Importantly, only ~50% of all tip–sample approaches encounter a PS I between the tip and the sample (for detailed statistics, see Supplementary Notes). Additional characterization with atomic force microscopy (Supplementary Fig. S4) confirmed a submonolayer coverage of PS I proteins in our experiment. Given the apex size of the SNOM tip, there is a probability of contacting two molecules, but this cannot be appreciable. For multiple contacts, one has to take into account different scenarios where two or more PS I proteins could be oriented parallel or antiparallel between the electrodes, either diminishing or adding to one another's photocurrent. The

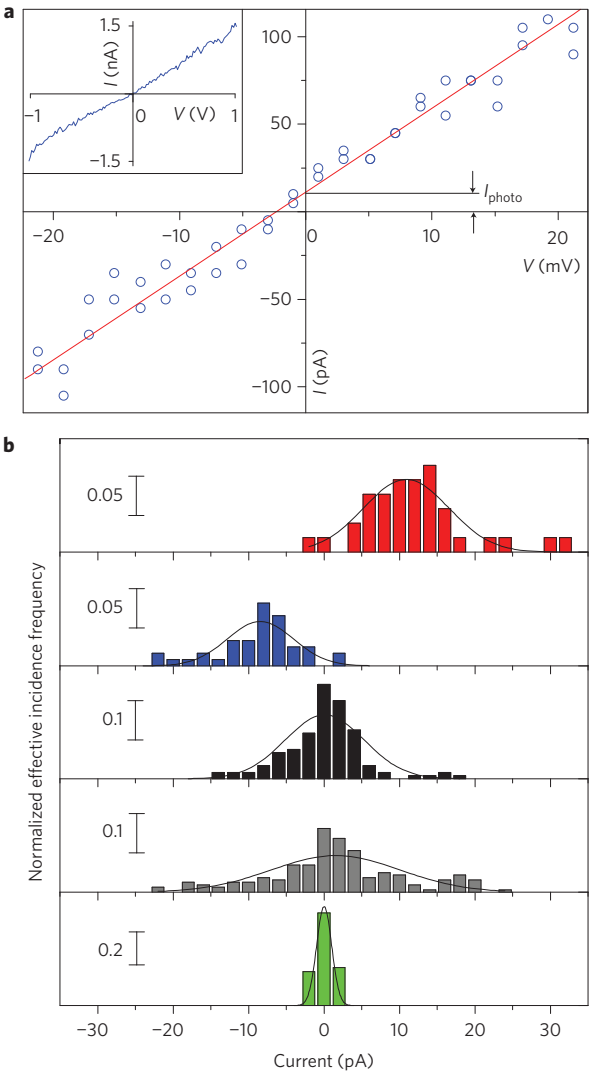

Figure 4 | Photocurrent analysis and histograms. a, Typical current–voltage dependence of bipolar PS I under laser excitation close to zero bias. The ordinate interception of the linear fit defines the residual current I_{photo} at zero bias (that is, 11±13 pA). Inset: dependence up to $|V_{bias}| = 1$ V. **b**, Compilation of photocurrent and reference measurements using individually prepared junctions with different PS I mutations and light exposure as indicated. Red: histogram of I_{photo} for different illuminated single bipolar PS I junctions, showing a positive offset when contacted (average photocurrent: 11±5.6 pA). Blue: photocurrent histogram of different illuminated single bipolar PS I junctions, showing a negative offset (average photocurrent: −8.4±4.4 pA). Black: reference data for different bipolar PS I junctions, without illumination (average residual current −0.09±5.3 pA). Grey: photocurrent histogram taken from different illuminated unipolar PS I molecules (average residual current: 1.54±8.57 pA). Green: residual current histogram for several measurements without photosystem, taken at a comparable tunnelling conductance and illumination of the tip (average current: 0.021±1.0 pA). Histogram heights are normalized according to the probability of their occurrence.

photocurrent contributions from the inter-electrode species might even vary and thus be partially hidden in the broadening of the histograms in Fig. 4. A careful analysis of our data for illuminated junctions containing bipolar PS I that showed no significant photocurrent did not lend any support to such scenarios. For unipolar PS I, we did not observe any significant short-circuit current (grey histogram). These findings suggest that to obtain an efficient electron transfer, the PS I should be covalently bound to both top and bottom electrodes, in accordance with recent studies on single molecules[4] and reaction centres[25]. Although a covalent bond is not mandatory to measure electron flow through a protein[11], in our experimental procedures the inability to recognize the first contact to the unipolar PS I in the approach provides an explanation for the inability to detect photocurrent for this species.

One of the most significant results in our experiment is the intriguingly large value of ∼10 pA for I_{photo}. This translates into a turnover time of ∼16 ns; in other words, every ∼16 ns, an electron transverses the PS I covalently bound between the two electrodes. As sketched in Fig. 2, a photoexcited electron reaches F_X in ∼15 ns at the earliest, equivalent to the rate we deduce from our photocurrent measurements. Therefore, the expected limiting step of the electron transfer—electron transfer from F_X to $F_{A/B}$—seems to be overcome by a direct transfer process to the covalently bound tip. This interpretation is consistent with the rather high dark currents of ∼1.5 nA at $V_{bias} \approx 1$ V (Fig. 4a, inset), which suggest that electron transfer to the top electrode is not limited by the second slower stage. In particular, our dark current values are consistent with results measured for a reaction centre coated gold tip[21]. The measured photocurrent, however, is higher than simple expectations based on the electron transfer rates of PS I in solution[26]. Recent studies demonstrate that the electron transfer in proteins in the dry state can be several orders of magnitude higher than in solution[27]. Assuming an internal quantum efficiency close to 1 (ref. 1) and absorption of the PS I monolayer of 0.003 at 633 nm, the electron transfer time of 16 ns suggests a photon flux of at least $\sim 2 \times 10^{10}$ s^{-1}. This value translates to a near-field intensity of ∼3.5 kW cm^{-2} at the apex of our SNOM tip, which is in good agreement with the laser power in our experiment after considering field enhancement effects. The photocurrent generated by a single PS I in our experiments corresponds to a current density of ∼0.15 mA cm^{-2} for 0.1 W cm^{-2} illumination with the given lateral dimensions of the PS I proteins.

Our results demonstrate that individual PS I units can be integrated and selectively addressed in nanoscale photovoltaic devices while retaining their biomolecular functional properties. They act as light-driven, highly efficient single-molecule electron pumps that can function as current generators in nanoscale electric circuits.

Received 29 March 2012; accepted 28 August 2012; published online 30 September 2012

References

1. Brettel, K. Electron transfer and arrangement of the redox cofactors in photosystem I. *Biochim. Biophys. Acta* **1318,** 322–373 (1997).
2. Metzger, R. M. Unimolecular electronics. *J. Mater. Chem.* **18,** 4364–4396 (2008).
3. Reichert, J. *et al.* Driving current through single organic molecules. *Phys. Rev. Lett.* **88,** 176804 (2002).
4. Salomon, A. *et al.* Comparison of electronic transport measurements on organic molecules. *Adv. Mater.* **15,** 1881–1890 (2003).
5. Guo, X. *et al.* Covalently bridging gaps in single-walled carbon nanotubes with conducting molecules. *Science* **311,** 356–359 (2006).
6. Akkermann, H. B. & de Boer, B. Electrical conduction through single molecules and self-assembled monolayers. *J. Phys. Condens. Matter* **20,** 13001 (2008).
7. Dulić, D. *et al.* One-way optoelectronic switching of photochromic molecules on gold. *Phys. Rev. Lett.* **91,** 207402 (2003).
8. Battacharyya, S. *et al.* Optical modulation of molecular conductance. *Nano Lett.* **11,** 2709–2714 (2011).
9. Wu, S. W., Ogawa, N. & Ho, W. Atomic-scale coupling of photons to single-molecule junctions. *Science* **312,** 1362–1365 (2006).
10. Van der Molen, S. J. *et al.* Light-controlled conductance switching of ordered metal–molecule–metal devices. *Nano Lett.* **9,** 76–80 (2009).
11. Lee, I., Lee, J. W. & Greenbaum, E. Biomolecular electronics: vectorial arrays of photosynthetic reaction centers. *Phys. Rev. Lett.* **79,** 3294–3297 (1997).
12. Das, R. *et al.* Integration of photosynthetic protein molecular complexes in solid-state electronic devices. *Nano Lett.* **4,** 1079–1083 (2004).
13. Frolov, L., Rosenwaks, Y., Carmeli, C. & Carmeli, I. Fabrication of a photoelectronic device by direct chemical binding of the photosynthetic reaction center protein to metal surfaces. *Adv. Mater.* **17,** 2434–2437 (2005).
14. Grätzel, M. Photoelectrochemical cells. *Nature* **414,** 338–344 (2001).

15. Ham, M. H. *et al.* Photoelectrochemical complexes for solar energy conversion that chemically and autonomously regenerate. *Nature Chem.* **2,** 929–936 (2010).
16. Blankenship, R. E. *et al.* Comparing photosynthetic and photovoltaic efficiencies and recognizing the potential for improvement. *Science* **332,** 805–809 (2011).
17. Carmeli, I. *et al.* A photosynthetic reaction center covalently bound to carbon nanotubes. *Adv. Mater.* **19,** 3901–3905 (2007).
18. Kaniber, S. M., Brandstetter, M., Simmel, F. C., Carmeli, I. & Holleitner, A. W. On-chip functionalization of carbon nanotubes with Photosystem I. *J. Am. Chem. Soc.* **132,** 2872–2873 (2010).
19. Carmeli, I. *et al.* Broad band enhancement of light absorption in Photosystem I by metal nanoparticle antennas. *Nano Lett.* **10,** 2069–2074 (2010).
20. Stamouli, A., Frenken, J. W. M., Oosterkamp, T. H., Cogdell, R. J. & Aartsma, T. J. The electron conduction of photosynthetic protein complexes embedded in a membrane. *FEBS Lett.* **560,** 109–114 (2004).
21. Zhao, J. W., Davis, J. J., Sansom, M. S. P. & Hung, A. Exploring the electronic and mechanical properties of protein using conducting atomic force microscopy. *J. Am. Chem. Soc.* **126,** 5601–5609 (2004).
22. Lukins, P. B. & Oates, T. Single-molecule high-resolution structure and electron conduction of Photosystem II from scanning tunneling microscopy and spectroscopy. *Biochim. Biophys. Acta* **1409,** 1–11 (1998).
23. Reiss, B. D., Hanson, D. K. & Firestone, M. A. Evaluation of the photosynthetic reaction center protein for potential use as a bioelectronic circuit element. *Biotechnol. Progr.* **23,** 985–989 (2007).
24. Tsutsui, M., Taniguchi, M. & Kawai, T. Single-molecule identification via electric current noise. *Nature Commun.* **1,** 138 (2010).
25. Ron, I., Friedman, N., Sheves, M. & Cahen, D. Enhanced electronic conductance across bacteriorhodopsin, induced by coupling to Pt nanoparticles. *J. Phys. Chem. Lett.* **1,** 3072–3077 (2010).
26. Mikayama, T. *et al.* The electronic behavior of a photosynthetic reaction center monitored by conductive atomic force microscopy. *J. Nanosci. Nanotechnol.* **9,** 97–107 (2009).
27. Ron, I., Pecht, I., Sheves, M. & Cahen, D. Proteins as solid-state electronic conductors. *Acc. Chem. Res.* **7,** 945–953 (2010).

Acknowledgements

This work was supported by the DFG via SPP 1243 (grants HO 3324/2 and RE 2592/2), COST-Phototech, the China Scholarship Council, the Nanosystems Initiative Munich (NIM), the Munich Center for Advanced Photonics (MAP), ERC Advanced Grant MolArt (no. 47299) and the Center of NanoScience (CeNS) in Munich. The authors thank A. Brenneis for technical assistance.

Author contributions

D.G. and H.B. performed the experiments and analysed the data. I.C. produced the PS I mutants and self-assembly techniques, and introduced the theory. A.W.H. supervised sample preparation. J.R. supervised the photocurrent experiments. S.M.K. prepared the PS I substrates. I.C., I.V.F., A.W.H. and S.S. performed preliminary atomic force microscopy and scanning tunnelling microscopy measurements. J.R. and I.C. conceived the study and co-wrote the paper with A.W.H., J.V.B. and I.V.F.

Additional information

Supplementary information is available in the online version of the paper. Reprints and permission information is available online at http://www.nature.com/reprints. Correspondence and requests for materials should be addressed to J.R. and I.C.

Competing financial interests

The authors declare no competing financial interests.